XVI International Conference on Computational Plasticity. Fundamentals and Applications
COMPLAS 2021
E. Oñate, D. Peric, M. Chiumenti and Eduardo de Souza Neto (Eds)

A COMPARATIVE STUDY OF MATERIAL HARDENING MODELS FOR FORMING OPERATIONS AND PREDICTION OF KINEMATIC HARDENING BY MEANS OF AN ANALYTICAL INDICATOR

USAMA AHMED*, REMI LAFARGE* AND ALEXANDER BROSIUS*

*Chair of Forming and Machining Processes (FF)
Technische Universität Dresden (TUD)
01069 Dresden, Germany
e-mail: usama.ahmed@tu-dresden.de, web page: http://www.tu-dresden.de/mw/if/ff

Keywords: Hardening models, sheet metal forming, kinematic indicator

Abstract: This publication is focused on comparing two different material hardening models i.e. purely isotropic and a mixed kinematic hardening model for the simulation of forming operations. The influence of nonlinear strain paths is investigated using deep drawing and strip tensile bending experiments and their comparison with numerical simulations. This comparison enables us to determine which of the two material models is more accurate for forming operations. Subsequently, the complex nonlinear strain paths are analyzed using an analytical indicator developed at the Chair of Forming and Machining Process, TU Dresden [1], to predict the influence of kinematic hardening by comparing the experimental results with a combined material hardening model as well as a purely isotropic material model. The analytical indicator illustrates the regions in deformed samples that are most affected by kinematic hardening and shows the difference in target values as a result of mixed and purely isotropic hardening law.

1 INTRODUCTION

The development of finite element modeling and analysis techniques over the last fifty years has enabled the rapid development of virtual process optimization and has been used to significantly reduce tool development and manufacturing costs. In the field of deep drawing, the use of simulations reduces the cost of tool development by allowing better prediction of the material flow, crack formation, or other aspects such as elastic recovery [2]. Forming operations are concerned with increasing process reliability, improving tool performance and reducing costs. The increase in quality requirements and the goal of reducing production time call for increasingly accurate simulations. A large number of complex material hardening models have been developed in the past with the sole aim of accurately predicting the material behavior during forming processes [3]. It is known that in certain forming processes such as deep drawing that involve nonlinear strain paths, isotropic modeling of strain hardening is often insufficient, especially in predicting the springback phenomenon as compared to more advanced models that integrate the kinematic effect [4]. Therefore, a combination of isotropic and kinematic hardening models must be employed to accurately predict this mechanism. Since these models require a large number of tests to include strain path changes, these mixed

hardening models should only be employed for materials exhibiting a considerable Bauschinger-effect and in situations involving nonlinear strain paths in order to limit costs.

Extensive research has previously been conducted to investigate the kinematic hardening influence on the deep drawing process [5]. Liao et al. [4] showed that the accurate prediction of springback is quite a crucial factor to design deep drawing tools. Most of the research carried out implements a combined nonlinear isotropic-kinematic hardening model [6], however, Lee et al. [7] also captured the springback phenomenon using a distortional hardening model. In addition to the existing conventional methods, Mousavi et al. [8] successfully developed macro-structured tools to limit the springback angles for materials exhibiting a significant kinematic hardening. Due to the complexity of material models with kinematic hardening, the large number of parameters required, and the testing effort required to obtain characteristic values, much simpler models are often used in industry [9]. The downside of these simpler models is that in certain complex configurations isotropic modeling of strain hardening is often incomplete compared to more advanced models that integrate the kinematic effect [4].

To evaluate the influence of kinematic hardening and to quantify the nonlinearity in strain paths, various indicators have been proposed by Schmitt et al. [10], Herault et al. [11] and Tekkaya et al. [3] etc. In this study, complex nonlinear strain paths are analyzed using an analytical indicator developed by Lafarge et. al [1]. This indicator, based on a simple isotropic simulation, should allow choosing an appropriate model, avoiding costly and potentially unnecessary tests. This indicator can be applied in early feasibility studies without the need for a complete material characterization in advance. In this way, the product launch risk and development costs can be minimized.

1.1 Material hardening models

It is common to divide the material hardening models into four categories that include isotropic hardening, kinematic hardening, isotropic-kinematic (combined) hardening, and finally distortive and oriental hardening models. According to Toledano [12], during isotropic yielding, the yield surface expands uniformly during plastic deformation, maintaining its shape and orientation. This model was one of the first for plastic deformation modeling and was introduced mainly by R. Hill [13]. According to Hill, as long as the deformation rate remains low, the crystal orientation remains random and the anisotropy is preserved. Figure 1 a) shows a graphical interpretation of this model.

As opposed to isotropic hardening that results in uniform expansion or contraction of the yield surface, the kinematic hardening model translates the yield surface as a consequence of the current stress state and the extent of the yield surface remains constant [14] as shown in Figure 1 b). In kinematic hardening, an increase in tensile yield strength due to tensile loading is accompanied by a reduction in compressive yield. The phenomenon that leads to an increase in yield strength in the direction of plastic flow while at the same time decreasing the yield strength in the opposite direction is known as the Bauschinger effect as illustrated in Figure 1 c). A simple quantification of the reduction in yield stress is provided by the Bauschinger parameter α, which is defined by the ratio of the maximum yield stress in the first load to the

yield stress reached at the subsequent load reversal. Neglecting the Bauschinger effect leads to an incorrect calculation of residual stresses and ultimately to an incorrect prediction of elastic recovery. Therefore, modeling a cyclic behavior that involves strain path reversal must capture the Bauschinger effect to accurately determine the springback behavior as shown by [15].

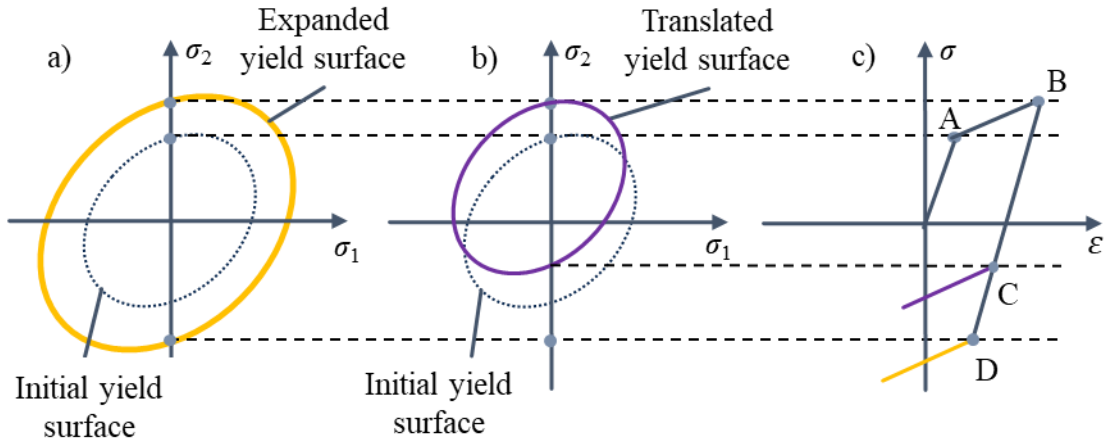

Figure 1: a) Isotropic hardening, b) kinematic hardening and c) Bauschinger effect in a stress-strain diagram

Kinematic hardening was first introduced by Prager [16] who introduced the term backstress. It is a homogeneous tensor to stress, called α, which represents the displacement of the flow surface. Several formulations have been proposed to parameterize the evolution of this tensor. The Prager model is linear, i.e., the relationship between the backstress tensor increments is proportional to the strain tensor increment. However, a pure kinematic model also fails to precisely capture the Bauschinger effect and therefore a combined hardening model consisting of an isotropic and kinematic hardening should be employed [17].

Combined hardening models combine the effects of several elementary models. For example, an isotropic-kinematic model includes isotropic (increase in yield surface) and kinematic (displacement of yield surface) hardening. Chaboche et al [18] proposed a combined strain hardening model and in the study [19], the authors propose another model known as the Yoshida or Yoshida-Uemori model. In this model, the authors considered two flow surfaces embedded in each other, called inner or flow and bounding surface. When the inner surface comes in contact with the bounding, it expands. Thus, the movement of the inner surface allows modeling the kinetic character of the flow, while the enlargement of the outer surface allows quantifying the isotropic strain relief. This model makes it possible to correctly model both the behavior of materials for high amplitude strains. Furthermore, the reversal of the load can explain the transient and permanent softening.

Although the mixed hardening models yield quite accurate results, they have a downside as well. The determination of material parameters in mixed hardening models is quite challenging and far more complex than for isotropic hardening. The material parameters are calculated by performing tension-compression tests. The complexity arises in the compression phase where buckling might occur in the sheet metal [20]. The buckling issue can be prevented by using

anti-buckling mechanisms that support the specimens on the surface, as well as by using miniaturized samples [21]. To limit cost, these mixed hardening models should only be employed for materials exhibiting a considerable Bauschinger-effect and in situations involving highly nonlinear strain paths

1.2 Kinematic hardening in deep drawing process

When a material is subjected to linear strain paths with no change in direction, the type of material hardening law makes no difference. Consequently, in a finite element simulation where all elements undergo a simple linear strain, kinematic hardening need not be considered. The deep drawing process on the other hand involves nonlinearity and strain path reversal due to the bending and unbending of the sheet along the die edge as shown in Figure 2. Since the non-linearity in the strain path can be influenced by other factors such as the tool's geometry, its quantification is not easily predictable and has nonuniform distribution in the sheet metal for the complex drawing process.

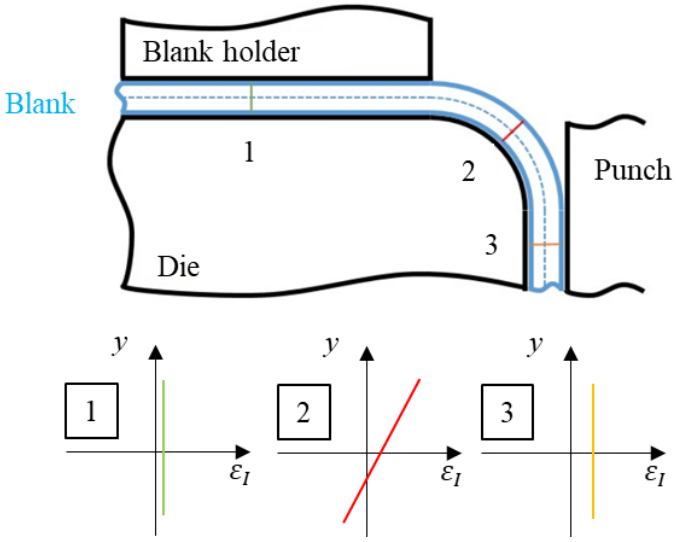

Figure 2: Strain reversal on die edge in deep drawing [1]

Oliveira et al. [9] investigated the kinematic hardening influence in U-profile forming process for mild and high strength steel i.e. DC06 and DP600 and concluded that nonlinearity in the strain path is linked to springback behavior. Further study is carried out by Liao et al. [4] to investigate the path-dependent behavior on twist springback in C-channel and P-channel. Their investigation led to the conclusion that the strain path has a substantial influence on springback simulations.

1.3 Analytical indicator for kinematic hardening:

The Kinematic Indicator used in this project is developed by Lafarge et. al [1]. According to [1], the indicator is proposed as:

$$I_{kin} = \sum \frac{\angle(\alpha, d\varphi_p) * \Delta W_p}{\pi * W_{p,max}} \quad (1)$$

Where:

- α is a reference for calculating the angle and is estimated as:

$$\dot{\alpha} = \frac{d\sigma_0}{d\varepsilon_{ep}^p} * \dot{\varphi}_p \quad (2)$$

- ΔW_p is the variation of the specific plastic work for the given timestep
- $W_{p,max}$ is the maximum of the specific plastic work in the part
- φ_p is the plastic strain and σ_0 the equivalent yield stress

To validate the use of this indicator, two simulations are carried out using LS-DYNA; one with a full isotropic model, and a second with a mixed model. The isotropic simulation results are used to calculate the indicator. Disparities between two simulations are then used as target values wherein the deviation between the two simulations is subsequently used as a measure of the influence of kinematic hardening. Different target variables may be used. This work focuses on specific accumulated plastic work and sheet thickness distribution. The calculation of the indicator is performed in Python using SciPy and the Python library qd.cae. For evaluation, different strain paths are analyzed, which are typical for deep drawing processes.

2 KINEMATIC HARDENING INFLUENCE IN STRIP TENSILE BENDING

Strip tensile bending experiments comprise a sheet metal strip that is placed between two high-strength clamps and undergoes tensile loading as well as bending along a cylindrical tool. In addition to the tensile force, a retention force is applied by the clamping jaws in the direction opposite to the tensile motion. The deformed samples show significant bending along the tool radius and can be used to investigate the springback.

The strip tensile bending experiments are undertaken to study two bending radii after the deformation for two different materials, DP600 steel and DP1000 steel. All experimental samples are deformed 100 mm in the drawing direction, caused by the hydraulic motion of clamping jaws. Strips of 210 mm x 20 mm are cut in the rolling direction and cutting edges were deburred. The cylindrical tool that represents the drawing edge is fixed in position but can rotate freely along the cylindrical axis. As a result, the influence of friction between the tool and the blank is minimized for the investigation. The tests are repeated five times to obtain an average value for the geometrical radius of deformed samples. For the calculation of geometric radii, a Python script is developed using the opencv library and recognizing the profile or 2D cross-section of the test specimens.

The strip tensile bending process is then simulated in LS DYNA Module 11.1.0 using MPP mode for parallel computation while implementing a pure isotropic and combined hardening model. The sheet blank is discretized with fully integrated shell elements (ELFORM = -16) with 9 integration points. To enable the calculation of the indicator, no mesh refinement is used. Barlat_YLD2000 (Mat_133) is used as the material model where the material parameters are identified utilizing tensile-compression and bulge tests for DP600 and DP1000. This material

card (Mat_133) implements Barlat 2002d Yield curve, an exponential hardening law for isotropic hardening, and a Chaboche model for kinematic hardening. The material parameters are given in Table 2.

Table 1: Strip tensile bending process parameters

	Sheet thickness [mm]	Tensile load [kN]	Retention load [kN]	Bending radius [mm]
Symbol	t	F_T	F_R	r
DP1000	1.5	2.60	1.71	30
DP600	1.0	1.95	1.64	30

Table 2: Material paramters of DP600 and DP1000 steel

	Elastic Modulus [Gpa]	Density Kg·m^{-3}	Swift Parameter	Swift Parameter [Mpa]	Swift Parameter	Kinematic hardening parameter
Symbol	E	ρ	ε_0	k	n	b
DP1000	171	7850	$2.0 \cdot 10^{-3}$	1209	$8.5 \cdot 10^{-2}$	0.42
DP600	160	7850	$2.6 \cdot 10^{-3}$	1069	0.18	0.32

For simplicity, the blank is pre-bent and translated along the direction of tensile loading as shown in Figure 3 a). A displacement of 100 mm is achieved using node-set displacement. Since the blank also experiences a retention load in a direction opposite to the tensile motion, this is accounted for by means of the application of load at the rear node-set.

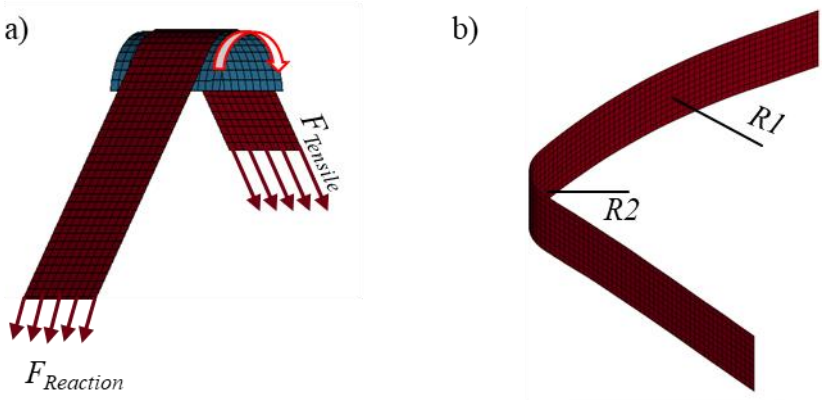

Figure 3: a) Strip tensile bending simulation set up and b) deformed sample after springback

The simulation of the forming process is followed by springback analysis to accurately measure the geometrical radii of deformed specimens. It requires creating an input deck for implicit springback using a dynain file and is achieved by INTERFACE_SPRINGBACK_LSDYNA keyword. The simulation history from the D3plot file in LS DYNA is import to Python script using qd.cae library after which the two geometrical angles are calculated for two material hardening models. The bar chart presented in Figure 4 shows radii measurements for DP600 and DP1000 and their comparison with experimental results.

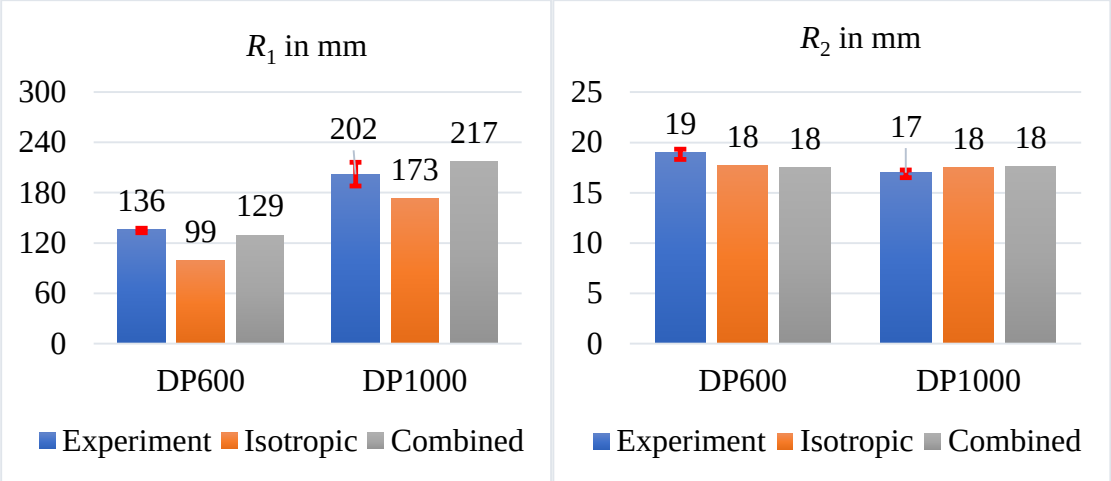

Figure 4: Measurements of geometrical radii for deformed strip tensile bending samples compared to simulated radii using different material models

R_1 represents the area that undergoes bending and unbending and is more prone to springback. So this region represented by R_1 is more likely to be influenced by kinematic hardening and is therefore of greater importance as compared to the region R_2. The simulation results in Figure 4 indicate that the combined hardening model shows very good agreement for R_1 with the experimental values as compared to isotropic hardening. For R_2, the difference between the calculations for the two hardening models is negligible, which is evident from the fact that this region is not governed by strain path reversal and therefore is not influenced by kinematic hardening.

The performance of the kinematic indicator is evaluated for strip tensile bending numerical simulations and is shown in Figure 5. The concept is that the regions with a high value of the indicator are more influenced by the kinematic hardening and vice versa. The larger values of the indicator are in the R_1 region i.e. the difference between the two material hardening models is quite significant because of the influence of kinematic hardening in this region. This result can also be observed from the bar chart in Figure 4, revealing large differences between purely isotropic and combined hardening models. In contrast, the indicator values in the R_2 region are quite small. It is because this region doesn't undergo strain path reversal and therefore kinematic hardening has a negligible influence and thus a smaller value of the kinematic indicator.

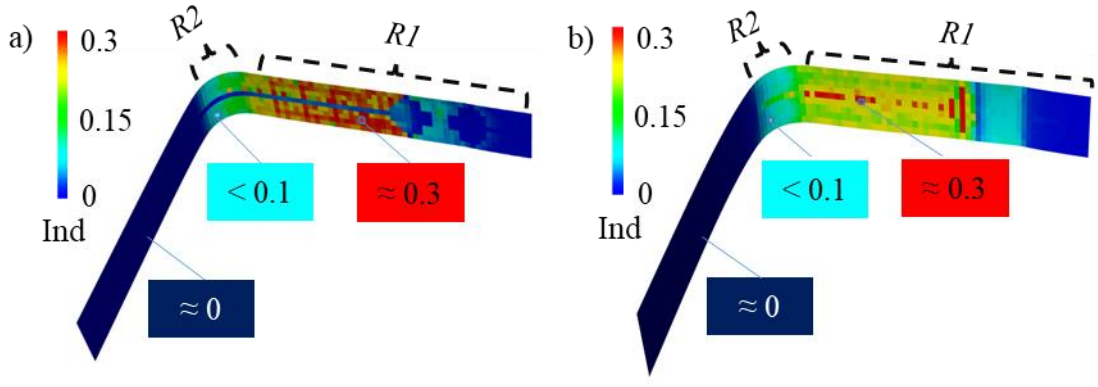

Figure 5: Kinematic indicator values in the upper layer of shell elements for a) DP600 and b) DP1000

3 KINEMATIC HARDENING INFLUENCE IN CROSS-CUP DEEP DRAWING

The second type of forming process implemented in this publication is the cross cup deep drawing. The experimental parameters are utilized to numerically simulate the process and measure sheet thickness distribution using an isotropic and mixed hardening material model. To validate the kinematic indicator, the sheet thickness distribution of numerically calculated components is compared with experimentally deep-drawn components. The cross-cup geometry is chosen because different strain states occur during the forming process. Thus, the accuracy of the indicator can be investigated at different strain states and possible imperfections can be highlighted.

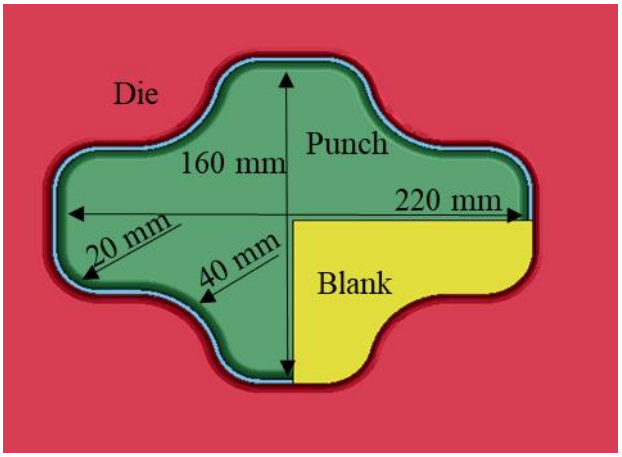

Figure 6: Cross cup deep drawing simulation model and the die geometry. The blank is only a quarter due to two symmetry planes

The forming process is carried out in a triple-acting hydraulic press Hydrap HDPZb 630 (Hydrap Pressen Maschinenbau GmbH & Co., Plüderhausen). The blank holder force for the production of components is adjusted so that wrinkling does not occur and high elongations are achieved in the process. Measures must be taken to reduce friction e.g. by using drawing oil

After the forming process, the components are measured and digitized using a strip light scanner. It is important here to measure both sides to be able to evaluate the sheet thickness locally.

The cross cup deep drawing simulation is performed using LS-DYNA with about 4300 fully integrated shell elements. Two symmetry planes are used to minimize computational time. The tool geometry and the schematic diagram of the cross cup simulation are shown in Figure 6. The simulations are performed and results are shown for DP600 steel with sheet thickness 1.0 mm drawn to a depth of 25 mm with a constant blank holder force of 400 kN. The calculations for DP600 steel are shown in Figure 7. The sheet thickness from the combined hardening model is very close to the experimental values for all areas. The comparison is also very good for the areas where the thickness is very low and are more prone to cracking.

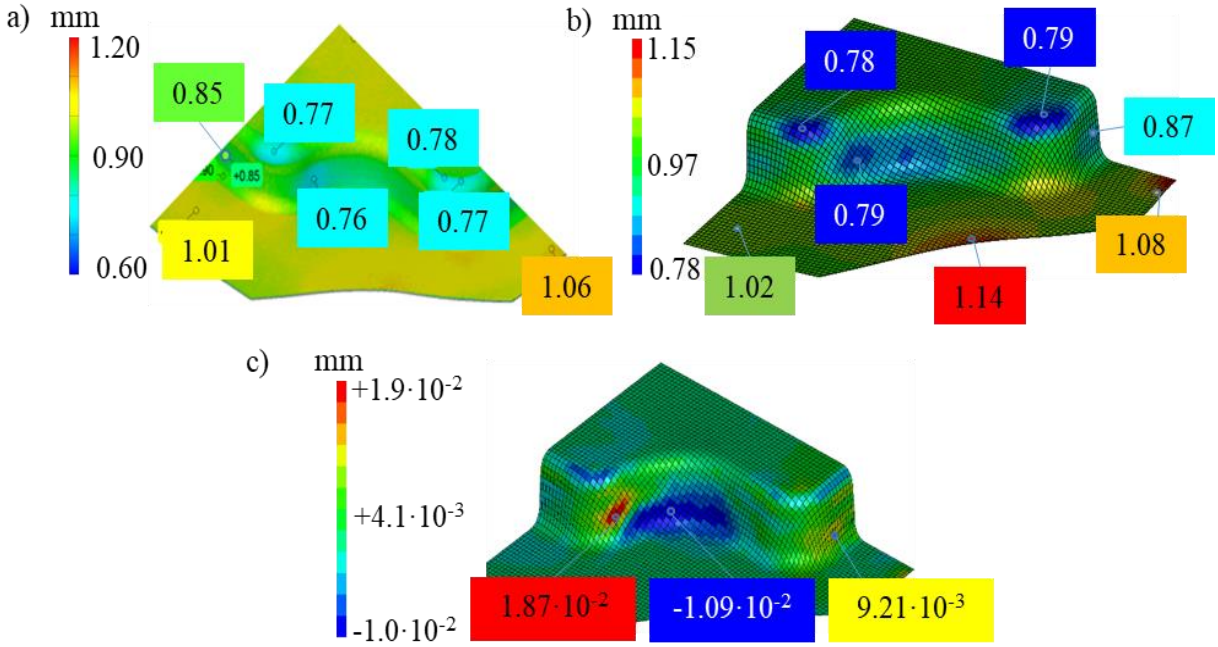

Figure 7: Comparison of plate thickness between (a) experimental results, (b) the combined material hardening model, and (c) the thickness difference between isotropic and combined strain hardening model for DP600.

The ability of the kinematic indicator to predict the regions affected by kinematic hardening is also shown in Figure 8. The objective is to show that high values of the indicator correlate with a strong influence of kinematic hardening. For deep drawing simulations, it is much easier to visualize this effect because the influence of kinematic hardening is more pronounced during bending and unbending in the process. The two target variables, equivalent plastic work and thickness of the blank at the end of the process are proposed for evaluation. Figure 8 presents a) indicator calculations at the last time step of the cross-cup simulation, b) specific plastic work, and c) difference of specific plastic work resulting from the two hardening models for DP600.

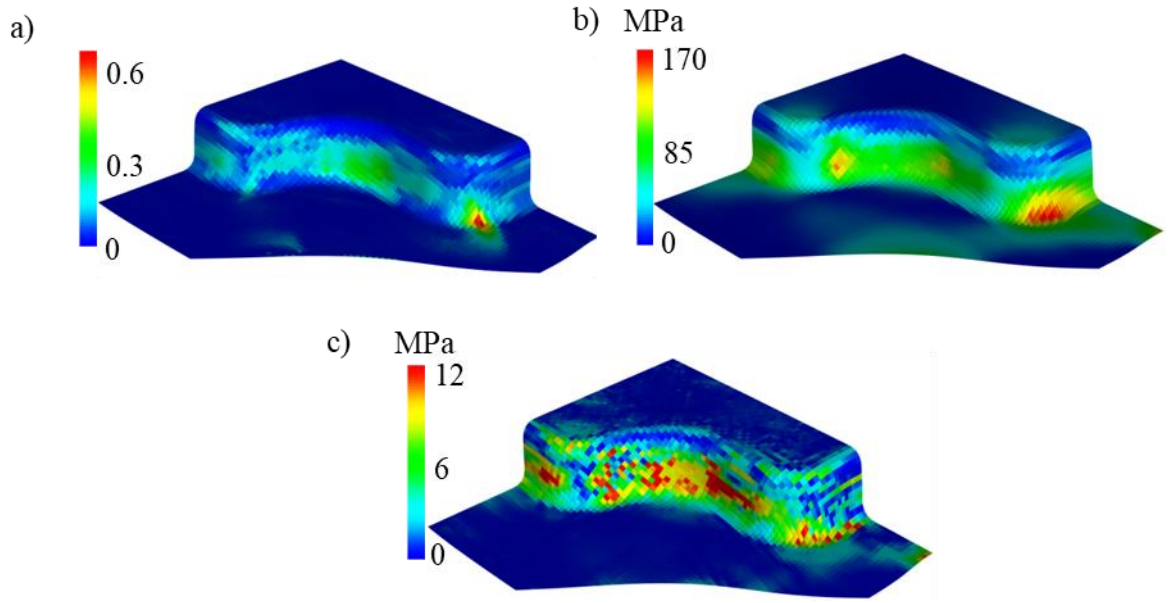

Figure 8: Illustration of the performance of the kinematic indicator for deep drawing of a cross cup in DP600. The figure represents a) Indicator calculation, b) Specific plastic work and c) Difference of plastic work

There is a good correlation between the values of the indicator and the error in the calculation of the kinematic hardening. The main working assumption of the indicator is that the drawing depths of the two simulations are as identical as possible. The bottom and top regions of the deformed cross-cup specimen show the negligible influence of kinematic hardening and are predicted appropriately by the kinematic indicator with comparatively low values. These areas also show little difference in sheet thickness between the two simulations. This is consistent with the fact that these regions undergo linear strain paths and are therefore not prominently influenced by kinematic hardening. Consequently, high values of the indicator correspond to areas that are significantly affected by kinematic hardening and therefore show higher differences between the two simulations. This is again consistent with the fact that these regions exhibit nonlinear behavior during deep drawing and undergo strain path reversal, making them more susceptible to the influence of kinematic hardening.

4 CONCLUSION

This study aims to propose simulation tools that help to select a material hardening model for the simulation of forming operations. Furthermore, the impact of nonlinear strain paths is investigated through strip tensile bending and deep drawing experiments. Subsequently, the complex nonlinear strain paths are analyzed utilizing an analytical indicator.

To begin with, experiments are conducted for strip tensile bending and deep drawing processes. These processes are then simulated in LS DYNA commercial code with two different material hardening laws that include full isotropic and a mixed kinematic hardening law. The geometrical properties measured from the experiments are then compared with both

simulated hardening models. It is followed by analyzing the influence of kinematic hardening utilizing an analytical indicator that shows the parts that are most influenced by the kinematic hardening. Similarly, the indicator shows the difference in target values as a result of isotropic and mixed hardening law.

The FE simulations show that results obtained from the mixed hardening material model better correspond to the experimental results for forming processes. The indicator, as well as the target values, show a significant sensitivity to regions that comprises nonlinear strain paths. The indicator calculations successfully predict the regions that are more prone to be influenced by kinematic hardening. Such regions are represented by higher and lower values of the kinematic indicator.

5 ACKNOWLEDGEMENT

The authors are grateful to the German Federation of Industrial Research Associations (AiF) for supporting the research project “Relevance analysis for the kinematic hardening in deep drawing processes with closed profiles" (IGF 19973BG). The computations were performed on a PC-Cluster at the Center for Information Services and High Performance Computing (ZIH) at TU Dresden.

REFERENCES:

[1] R. Lafarge, N. Küsters, and A. Brosius, “A novel indicator for kinematic hardening effect quantification in deep drawing simulation,” *COMPLASS Conf.*, pp. 1–12, 2019.

[2] A. Birkert, S. Haage, and M. Straub, *Umformtechnische Herstellung komplexer Karosserieteile*. Springer Vieweg, 2013.

[3] S. Bruschi *et al.*, “Testing and modelling of material behaviour and formability in sheet metal forming,” *CIRP Ann. - Manuf. Technol.*, vol. 63, no. 2, pp. 727–749, 2014, doi: 10.1016/j.cirp.2014.05.005.

[4] J. Liao, X. Xue, M. G. Lee, F. Barlat, G. Vincze, and A. B. Pereira, “Constitutive modeling for path-dependent behavior and its influence on twist springback,” *Int. J. Plast.*, vol. 93, pp. 64–88, 2017, doi: 10.1016/j.ijplas.2017.02.009.

[5] B. Haddag, T. Balan, and F. Abed-Meraim, “Investigation of advanced strain-path dependent material models for sheet metal forming simulations,” *Int. J. Plast.*, vol. 23, no. 6, pp. 951–979, 2007, doi: 10.1016/j.ijplas.2006.10.004.

[6] A. Taherizadeh, A. Ghaei, D. E. Green, and W. J. Altenhof, “Finite element simulation of springback for a channel draw process with drawbead using different hardening models,” *Int. J. Mech. Sci.*, vol. 51, no. 4, pp. 314–325, 2009, doi: 10.1016/j.ijmecsci.2009.03.001.

[7] J. Y. Lee, J. W. Lee, M. G. Lee, and F. Barlat, “An application of homogeneous anisotropic hardening to springback prediction in pre-strained U-draw/bending,” *Int. J. Solids Struct.*, vol. 49, no. 25, pp. 3562–3572, 2012, doi: 10.1016/j.ijsolstr.2012.03.042.

[8] A. Mousavi, K. S. Ridolfi, and A. Brosius, “Influence of alternating bending on springback behavior of parts in deep drawing process with macro-structured tools,” *MATEC Web Conf.*, vol. 190, pp. 1–5, 2018, doi: 10.1051/matecconf/201819014005.

[9] M. C. Oliveira, J. L. Alves, B. M. Chaparro, and L. F. Menezes, “Study on the influence of work-hardening modeling in springback prediction,” *Int. J. Plast.*, vol. 23, no. 3, pp. 516–543, 2007, doi: 10.1016/j.ijplas.2006.07.003.

[10] J. H. Schmitt, E. Aernoudt, and B. Baudelet, “Yield loci for polycrystalline metals without texture,” *Mater. Sci. Eng.*, vol. 75, no. 1–2, pp. 13–20, 1985, doi: 10.1016/0025-5416(85)90173-9.

[11] D. Herault, S. Thuillier, P. Y. Manach, and J. L. Duval, “Strain path changes in Reverse Redrawing of DP Steels,” *IOP Conf. Ser. Mater. Sci. Eng.*, vol. 418, no. 1, 2018, doi: 10.1088/1757-899X/418/1/012042.

[12] J.-C. Tolédano, *Physical basis of plasticity in solids*. 2011.

[13] H. Geiringer, “Review: R. Hill, The mathematical theory of plasticity,” *Bull. Amer. Math. Soc.*, vol. 58, no. 4, pp. 507–512, 1952.

[14] P. D. Pattillo, “Chapter 6 - Yield and Inelastic Behavior,” P. D. B. T.-E. of O. and G. W. T. D. Pattillo, Ed. Gulf Professional Publishing, 2018, pp. 151–195.

[15] M. Choteau, “Caractérisation de l’effet Bauschinger en sollicitations uniaxiales d’un acier inoxydable austénique X2CrNiM017-12-2,” 1999.

[16] W. Prager, “Recent developments in the mathematical theory of plasticity,” *J. Appl. Phys.*, vol. 20, no. 3, pp. 235–241, 1949, doi: 10.1063/1.1698348.

[17] B. K. Chun, J. T. Jinn, and J. K. Lee, “Modeling the Bauschinger effect for sheet metals, part I: theory,” *Int. J. Plast.*, vol. 18, no. 5, pp. 571–595, 2002, doi: https://doi.org/10.1016/S0749-6419(01)00046-8.

[18] J. L. Chaboche, K. Dang Van, and G. Cordier, *Modelization of the strain memory effect on the cyclic hardening of 316 stainless steel*. Netherlands: North-Holland Publishing Co, 1979.

[19] F. Yoshida and T. Uemori, “A model of large-strain cyclic plasticity describing the Bauschinger effect and workhardening stagnation,” *Int. J. Plast.*, vol. 18, no. 5, pp. 661–686, 2002, doi: https://doi.org/10.1016/S0749-6419(01)00050-X.

[20] R. K. Boger, R. H. Wagoner, F. Barlat, M. G. Lee, and K. Chung, “Continuous, large strain, tension/compression testing of sheet material,” *Int. J. Plast.*, vol. 21, no. 12, pp. 2319–2343, 2005, doi: 10.1016/j.ijplas.2004.12.002.

[21] D. Staud and M. Merklein, “Zug-Druck-Versuche an Miniaturproben zur Erfassung von Parametern für kinematische Verfestigungsmodelle,” in *Werkstoffprüfung 2009: Fortschritte der Kennwertermittlung in Forschung und Praxis*, vol. 2, G. G. M. Borsutzki, Ed. Düsseldorf: Verlag Stahleisen, 2009, pp. 211–218.